Shear Capacity and Mechanical Properties of Reactive Powder Concrete T-Beams

Prof. Dr. Hisham Mohamad Ali
Building and Construction Department
University of Technology/Baghdad

Asst. Prof. Dr. Jamal **Saeed** *abd alamir*
civil Engineering College
Al-Mustansiriyah University /Baghdad

Lecturer . Nagham Tariq Hamad
Highway & Transportation Engineering Department
Al-Mustansiriyah University /Baghdad

Abstract

Seven tests were conducted on RPC T- beams with three steel fiber-volume fractions (0, 1, and 2%), three shear span-depth ratios (a/d) (2.5, 3.5, and 4.3), and three silica fume percentage (SF) (15, 20 and 25%).

Based on observed data from the present experimental tests and other investigations, non-linear regression models are proposed for predicting the compressive strength (f'_{cf}) , splitting tensile strength (f_{spf}) and modulus of rupture (f_{rf}) of RPC . in addition , an equation is also proposed for the prediction of the shear capacity(V_u) of RPC T-sections. The accuracy of the proposed equations are examined by comparison with similar existing equations and available experimental results.

Keywords: shear capacity, Reactive Powder Concrete& Tee Beams

سعة القص والخواص الميكانيكية لعتبات خرسانة المساحيق الفعالة ذات مقطع T-

أ.د.هشام محمد علي
قسم هندسة البناء والإنشاءات
الجامعة التكنولوجية

أ.م.د. جمال سعيد عبد الامير
قسم الهندسة المدنية
الجامعة المستنصرية

م. نغم طارق حمد
قسم هندسة الطرق والنقل
الجامعة المستنصرية

الخلاصة :

أجريت اختبارات على سبعة عتبات خرسانية لخرسانة المساحيق الفعالة ذات مقطع T وتم استخدام ثلاثة نسب لحجم الألياف الفولاذية (0، 1، و 2٪)، ثلاثة نسب لفضاء القص إلى العمق الفعال (a/d) (2.5، 3.5، و 4.3)، وثلاثة نسب لمحتوى السيليكا الفعالة (SF)، (15و20و25٪).

واستنادا إلى البيانات التي تم الحصول عليها من الاختبارات التجريبية الحالية ونتائج تجريبية لباحثين آخرين ، تم اقتراح نماذج لتخمين مقاومة الانضغاط (f'_{cf})، مقاومة الانفلاق (f_{spf}) ومعامل الكسر (f_{rf}) لخرسانة المساحيق الفعالة. وبالإضافة إلى ذلك، تم إجراء اشتقاق نظري لإيجاد الحمل الأقصى Vu للعتبات الخرسانية ذات مقطع T- لخرسانة المساحيق الفعالة الخالية من الأطواق استنادا إلى تقنية تحليل الارتداد (regression analysis). وقد تم فحص دقة المعادلات المقترحة بالمقارنة مع معادلات موجودة مماثلة والنتائج التجريبية المتاحة.

1. Introduction

Reactive powder concrete (RPC) is a cementitious material that exhibits high-performance properties such as limited shrinkage and creep, low permeability, ultra-high strength and increased protection against corrosion. The properties of RPC make it a revolutionary material in the field of concrete technology with possibilities for use in a wide range of structural and non-structural applications[1]. RPC is characterized by high strength and very low porosity, which is obtained by optimized particle packing and low water content. It has capacity to deform and support flexural and tensile loads, even after initial cracking. The durability properties are those of an impermeable material, there is almost no penetration of chlorides and sulphates and high resistance to sulphate attack. Resistance to abrasion is similar to that of rock. The development of RPC has the potential to revolutionize design in precast, prestressed, concrete[1]. Currently, to achieve excellent mechanical behavior, some special techniques and raw materials must be adopted in the preparation of UHPC, which include:

a. Coarse aggregate is removed to enhance the homogeneity of concrete.
b. Metal fiber or steel tube is introduced to improve ductility of composites.
c. High quality superplasticizer and large quantities of superfine silica fume and quartz are added to achieve a low water/binder ratio to reduce porosity and improve strength.
d. Pressure may be applied before and during the setting to increase the compactness of the concrete.
e. High activity micro-silica and/or precipitated silica may be mixed into cementitious materials to accelerate the hydration of cement and catalyze a strong pozzolanic reaction effect.
f. Steam curing may be supplied to gain higher strength.

2. Variables and Specimen Dimensions

The experimental program included casting and testing seven RPC T-beams without steel stirrups. The specimens were designed to fail by diagonal tension (shear) in the web region.

The main variables studied in the experimental program were

- Volume fraction of steel fibers(V_f)
- Percentage of silica fume (SF)
- Shear span-to-depth ratio(a/d)

All tested beams were simply supported and subjected to two point loads **Figure.(1).** Each beam had 1300 mm total length and 1200 mm span between the supports. The beam dimensions and details are shown in **Figure. (1) and Table (1).**

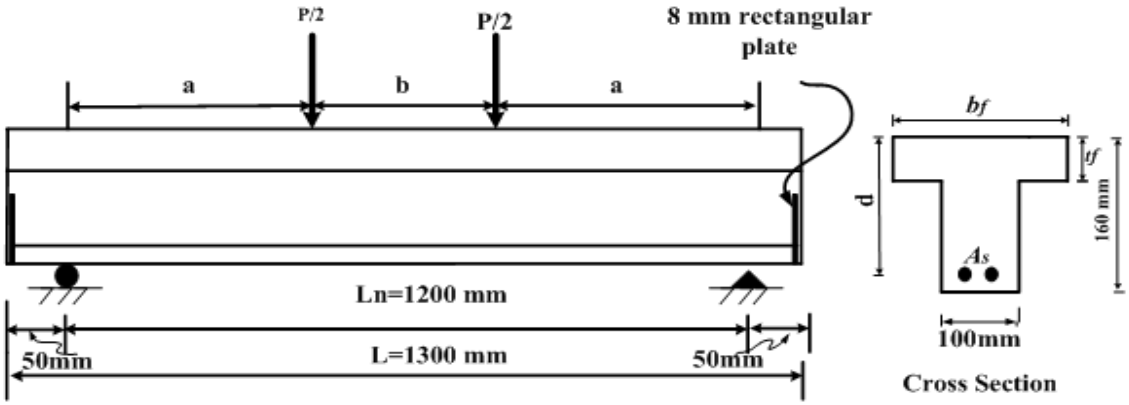

Fig .(1): Details of a Typical Test Beam.

Table .(1): Beam Groups and Concrete Properties.

Group	Beam No.	V_f%	a/d	SF%	ρ_w%
Change in V_f	1	0	3.5	25	7.7
	2	1	3.5	25	7.7
	3	2	3.5	25	7.7
Change in a/d	3	2	3.5	25	7.7
	4	2	2.5	25	7.7
	5	2	4.3	25	7.7
Change in SF	3	2	3.5	25	7.7
	6	2	3.5	20	7.7
	7	2	3.5	15	7.7

3. Material, Mix Design and Fabrication

Details of the RPC mixes for specimens B1 to B7 are given in **Table (2**). The cement used in this project was Tasluoja Ordinary Portland cement Type 1. General Portland cement used conformed to the Iraqi specification No.5 / 1984. [2]

The silica fume used was with particle size range between 150 μm and 400 μm. The superplasticizer used in the mix was Flocrete PC 260, which is a polycarboxylic ether based superplasticizer. The fibers were straight 13 mm long by 0.2 mm diameter and are fabricated from very high strength steel with minimum tensile strength of 1800 MPa. Three fiber volume ratios (V_f) were used 0, 1 and 2 %.

The mix type M0,25 was adopted as a reference mix which had no steel fibers and 25% silica fume ratio. The five types of RPC mixes of Table (2) were used to cast the main beam specimens in the present investigation as well as their control specimens.

All the dry components (i.e. cement, silica fume and sand) were pre-batched into 0.5 tone bags. The dry components were then transported to the high energy mixer and mixed for about 10 minutes. Water and superplasticizer were added gradually until the materials were uniformly mixed. The fibers were introduced last, dispersed uniformly and mixing continued for a further 2-3 minutes. All specimens were cast vertically in steel forms as shown in **Plate 1**. The forms were cleaned and greased to allow smooth stripping. The fresh RPC was compacted using external vibrators which were attached to the steel forms. Within one hour of casting, the specimens and test control samples were covered under plastic nylon until the day of demoulding. After stripping at age 1 day, the specimens were cured for 2 days at 80°C in a hot water bath. At age 3 days the specimens were removed from the hot water bath and stored in water at 25°-30° C for 28 days then stored in the laboratory until the time of testing.

Table .(2): Properties of the Different Types of RPC Mixes.

Mix Type	Beam No.	Cement kg/m3	Sand kg/m3	Silica fume* %	Silica fume kg/m3	w/c	Flocrete PC 260** %	Steel fiber content*** %	Steel fiber content kg/m3
M0,25	B1	1000	1000	25	250	0.2	3.0	0	0
M1,25	B2	1000	1000	25	250	0.2	3.0	1	78
M2,25	B3,B4,B5	1000	1000	25	250	0.2	3.0	2	156
M2,15	B7	1000	1000	15	150	0.2	3.0	2	156
M2,20	B6	1000	1000	20	200	0.2	3.0	2	156

* Percent of cement weight.

** Percent of binder (cement + silica fume) weight.

*** Percent of mix volume.

Plate .(1): casting and curing of specimens

4. Test Setup and Instrumentation

All beams and control specimens were removed from the curing water tank at age of 28 days. Before testing, the beam was cleaned and painted white to allow easy detection of crack propagation. The demec points were placed in position on the beam. The beam was placed on its supports in the machine with a clear span of 1200 mm. Loading was applied through steel

plates to avoid stress concentration on the beam flange. The test of the PRC T-beam is shown in **Plate (2**).

All beams were tested under two points loading. The dial gage was placed in its position touching the bottom surface of the beam at mid-span. Before loading was applied, the zero-load readings of the mechanical strain gages as well as the dial gage were taken and then a load of 5 kN was applied and released in order to recheck the zero-load readings.

The magnitude of the load at every single step of loading was chosen according to the expected strength of the beam. At each load value, concrete surface strains and the dial gage reading were recorded and a search was made for the appearance of the cracks by using a magnifying glass. The positions and extents of the first and the other consequent cracks were marked on the surface of the beam and the magnitude of the applied load at which these cracks occurred was recorded. The inclined cracking load was reported as being the load causing the critical diagonal crack to cross the mid-depth of the beam. The beam was considered to reach failure when it showed a drop in loading with increasing deformation. The failure load was thus recorded, and the load was then removed to allow taking some photographs of the final crack pattern.

Plate .(2): Testing RPC T-Beam

5. Mechanical properties

The results of the material control tests are summarized in **Table (3)** the mean compressive strength (f'_{cf}) was determined from six 200 mm high by 100 mm diameter cylinders stressed under load control at a rate of 20 MPa per minute. The ends of the cylinders were ground flat. The modulus of elasticity (E_o) was obtained from stress-strain tests on 200 mm high by 100 mm diameter cylinders The tensile strength of the material was evaluated using split cylinder (Brazil) tests. The split cylinder tensile strength (fsp_f) was obtained from tests on six 200 mm high by 100 mm diameter cylinders loaded at 1.0 MPa per minute via a 10 mm wide loading strip. The two point flexural tension strength (f_{rf}) was obtained from 100 mm square prisms spanning 500 mm to find modulus of rupture.

Table .(3) Properties of Hardened RPC.

Type of mix	Fiber content(V_f)%	Silica Fume SF%	Compressive Strength $f'cf$ (MPa)	Splitting Tensile Strength $fspf$ (MPa)	Modulus of Rupture frf (MPa)	Modulus of Elasticity Ec (GPa)
M0,25	0	25	101	5	5.2	44.94
M1,25	1	25	127	14.7	15.3	50.52
M2,25	2	25	148	19.8	21	54.72
M2, 20	2	20	139	17.3	19	52.90
M2,15	2	15	130	16.4	18.6	51.13

6. Test results and observations

The experimental results of the shear tests are summarized in **Table (4)** where *Vcr* is the force at which the first shear cracking was detected visually on the specimen and *Vu* is the maximum force recorded during the experiments.

Table .(4): Details of Cracking and Ultimate Shear Strength for Tested Beams.

beams	V_f %	ρ_w	SF %	a/d	f'_{cf} (MPa)	Shear strength (kN)		$\frac{V_{u,test}}{V_{cr,test}}$	Mode of failure
						V_{cr}	V_u		
B1	**0**	**0.077**	**25**	**3.5**	**101.0**	**25.0**	**45.25**	**1.81**	**DT**
B2	**1**	**0.077**	**25**	**3.5**	**127.0**	**30.0**	**70.50**	**2.35**	**DT**
B3	**2**	**0.077**	**25**	**3.5**	**148.5**	**40.0**	**122.75**	**3.07**	**DT**
B4	**2**	**0.077**	**25**	**2.5**	**148.5**	**45.0**	**209.5**	**4.66**	**DT**
B5	**2**	**0.077**	**25**	**4.3**	**148.5**	**30.0**	**100.0**	**3.33**	**DT**
B6	**2**	**0.077**	**20**	**3.5**	**139.0**	**37.5**	**119.25**	**3.18**	**DT**
B7	**2**	**0.077**	**15**	**3.5**	**130.0**	**35.0**	**111.5**	**3.19**	**DT**

DT: Diagonal tension failure.

7. Regression Equation for RPC Properties

7.1 Compressive Strength

Regression models are proposed in the present work based on (84) experimental data points obtained from this investigation and other investigations given in Appendix, by using the trial version 9 of DtatFit software of Oakdale Engineering. The data used represents a wide range of fiber factor and compressive strength (62.6 - 231) MPa. The proposed expressions for predicting the compressive strength of RPC are given by Eq. (1) as follows;

$$f'_{cf} = 1.4\, f'_c\, F^{0.05} \qquad \text{..... (1)}$$

where

f'_{cf} = compressive strength of fibrous RPC, MPa

$f'c$ = compressive strength of nonfibrous RPC, MPa

F = fiber factor given by: $\boldsymbol{F = \frac{l_f}{d_f} V_f B_f}$

To test this equation, the relative compressive strengths ($\boldsymbol{f'_{cf}}$ ***test/*** $\boldsymbol{f'_{cf}}$ ***proposed***) was found using for the (84) test results listed in Appendix. The values of the mean (μ) , standard deviation (SD) and coefficient of variation (COV) are 0.992573 , 0.111683 and 11.25% respectively.

Figure(2) shows tests values versus proposed values of f'_{cf} for (84) test results using Eq.(1).

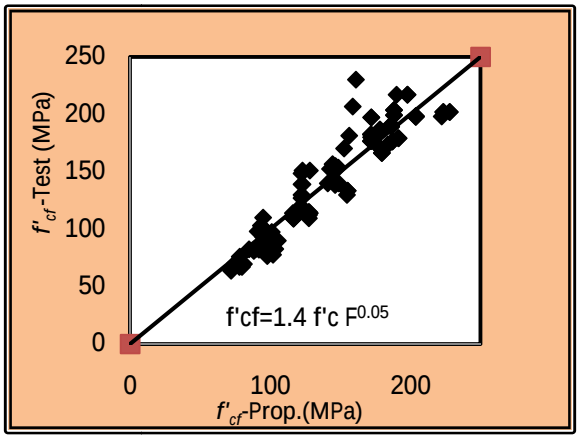

Fig .(2) :Test Values Versus Proposed Values of Compressive Strength RPC Using Eq. (1).

7.2 Splitting Tensile Strength

Regression models are developed in the present research based on (54) experimental data points obtained from this investigation and other investigations given in Appendix. The proposed expressions for predicting the splitting tensile strength of RPC are given by Eq. (2) as follows ;

$$\boldsymbol{f_{spf} = 0.14\, f'_{cf}\, F^{0.08}} \qquad \text{.....(2)}$$

To test this equation, the relative splitting tensile strength ($\boldsymbol{f_{spf}}$ ***test/*** $\boldsymbol{f_{spf}}$ ***proposed***) was found for the (54) test results. The values of the mean (μ), standard deviation (SD) and coefficient of variation (COV) are 0.99 , 0.154 and 15.52% respectively.

Figure(3) shows tests values versus proposed values of f_{spf} for (54) test results using Eq. (2).

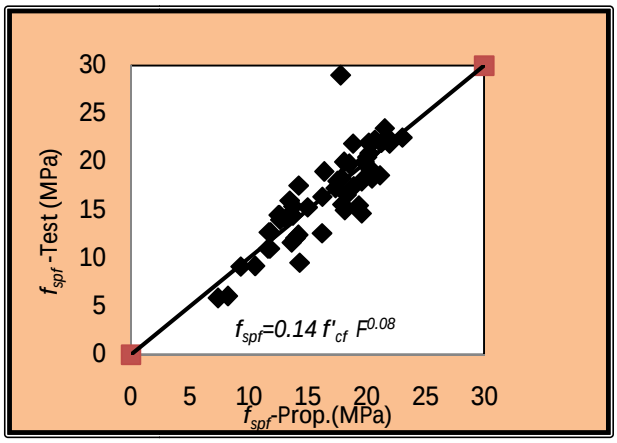

Fig .(3) :Test Values Versus Proposed Values of Splitting Tensile Strength RPC using Eq. (2).

7.3 Modulus of Rupture

The modulus of rupture of RPC, (f_{rf}), is a function of fibrous compressive strength and fiber factor. The constants were calculated by a regression analysis using (74) experimental data points obtained from this investigation given in the Appendix. The data used represents a wide range of fiber content in compressive strength (67.3 - 214.7) MPa. The proposed equations for predicting modulus of rupture of RPC are given by Eq. (3) as follows;

$$f_{rf} = 0.03 \left(f'_{cf}\right)^{1.3} F^{0.004} \qquad \text{.....(3)}$$

To test this equation, the relative modulus of rupture (***frf test/ frf proposed***) was found using each of those expressions for the (74) test results. The values of the mean (μ) , standard deviation (SD) and coefficient of variation (COV) are 1.04, 0.107 and 10.3% respectively. **Figure. (4)** shows tests values versus proposed values of f_{rf} for (74) test results using Eq. (3).

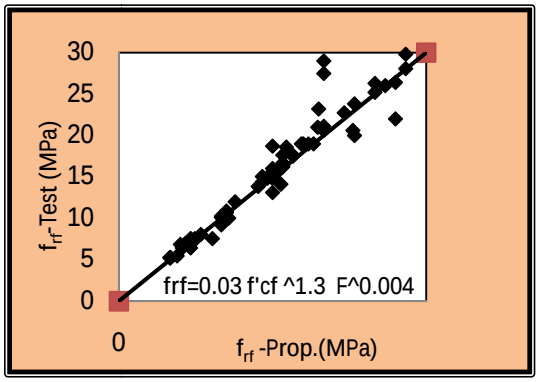

Fig. (4): Tests Values Versus Proposed Values of Modulus of Rupture RPC Using Eq. (3).

8. Shear Strength of T-Beams:

The shear resistance of reinforced concrete beams has been a well-known research subject over the last several decades. The study of shear resistance in the case of T-beams, however, is limited. In international codes, such as the ACI Building Code and the Eurocode, the shear force in a T-beam is assumed to be carried only by its web. This simplified assumption, however, which has prevailed in the shear design practice, is not correct. The tests show that the shear strength of T-beams is, in many cases, considerably higher than the one of the rectangular beams of its web.

In 2001, Zararis and Papadakis [3] proposed a theory to describe the shear failure in ordinary slender rectangular beams (that is, beams with a shear span to depth ratio (a/d) greater than 2.5) with or without shear reinforcement.

This theory was developed later by Zararis, L.P. and Zararis, P.D. [4] (2006) to describe the shear failure of slender T-beams. According to this developed theory, an analytical expression was obtained for determining the ultimate shear capacity of reinforced concrete slender T-beams under concentrated load by using a suitable effective width.

In the present work, the Zararis and Zararis theory's is extended to establish an equation for determining the ultimate shear capacity of RPC slender T-beams under two- concentrated load. This equation is then used to explain, in a rigorous and consistent way, the experimentally observed behavior of T- beams failing in shear.

9. Shear Strength of Rectangular and T- Beams without shear Reinforcement Overview :

In normal slender rectangular-beams without shear reinforcement, the critical diagonal crack is caused by a type of splitting of concrete in the compression zone as shown in Figure(5), according to which the stress distribution along the line of splitting is not similar to the one occurring in the common split cylinder test.

The theory [3, 4] results in the simple expression:

$$V_{u=}\left(1.2-0.2\,\frac{a}{d}\,d\right)\frac{c}{d}\,f_{sp}\,b_w\,d \qquad \text{..... (4)}$$

where:

$$\left(1.2-0.2\,\frac{a}{d}\,d\right)\geq 0.65 \quad (d\ in\ meters) \text{ is the size effect} \qquad \text{..... (5)}$$

Vu = ultimate shear force of slender beam without shear reinforcement.
a/d =shear span to depth ratio
d = effective depth of the section.

c/d = ratio of the neutral axis depth to the effective depth of section

f_{sp} = splitting tensile strength of concrete (MPa).

b_w =width of web.

The depth $\boldsymbol{c}$ of the compression zone in Eq. (4) is given by:

$$\left(\frac{c}{d}\right)^2 + 600\frac{\rho}{f'_c} * \frac{c}{d} - 600\frac{\rho}{f'_c} = 0 \qquad \ldots\ldots\ldots\ldots\ldots\ldots (6)$$

where: ρ = steel ratio , f'_c = strength of concrete in MPa.

In the case of T-beams the width of the area where the splitting of concrete occurs is not remaining constant, but it is changing from the width b_w of the web to the width b_f of the flange.

As it was shown in the crack pattern of the upper part of the of the T-beams as show in Plate 3, the inclined cracks on the flange of the T-beams imply that the stresses in the flange are limited in an area, the width of which changes almost linearly from b_w to b_f. defining as " effective width " of a T- beam in shear $bef = A/c$, where $\boldsymbol{A}$ equals the area of the shaded part of the cross section, and c equals the distance from extreme compression fiber to neutral axis(depth of compression zone), as show in **Figure.(6).** The following expression was derived

$$\boldsymbol{b_{ef}} = \boldsymbol{b_w}\left[1 + \boldsymbol{o.5} * \frac{\boldsymbol{t_f}}{\boldsymbol{d}}\left(\frac{\boldsymbol{b_f}}{\boldsymbol{b_w}} - 1\right) / \frac{\boldsymbol{c}}{\boldsymbol{d}}\right] \qquad \ldots\ldots\ldots\ldots\ldots\ldots \textbf{(7)}$$

The ultimate shear strength of T-beams without shear reinforcement, becomes

$$\boldsymbol{V_u} = \left(\boldsymbol{1.2 - o.2}\,\frac{\boldsymbol{a}}{\boldsymbol{d}}\,\boldsymbol{d}\right) * \frac{\boldsymbol{c}}{\boldsymbol{d}}\,\boldsymbol{f_{sp}}\,\boldsymbol{b_{ef}}\,\boldsymbol{d} \qquad \ldots\ldots\ldots\ldots\ldots\ldots \textbf{(8)}$$

And the depth $\boldsymbol{c}$ of the compression zone in Eq.(8) was determined analytically after taking into account the shape of the compression zone as:

$$\left(\frac{\boldsymbol{c}}{\boldsymbol{d}}\right)^2 + \left[\boldsymbol{1.5}\,\frac{\boldsymbol{t_f}}{\boldsymbol{d}}\left(\frac{\boldsymbol{b_f}}{\boldsymbol{b_w}} - 1\right) + \boldsymbol{600}\frac{\boldsymbol{\rho}}{\boldsymbol{f'_c}}\right] * \left(\frac{\boldsymbol{c}}{\boldsymbol{d}}\right) - \boldsymbol{600}\frac{\boldsymbol{\rho}}{\boldsymbol{f'_c}} = \boldsymbol{0} \qquad \ldots\ldots\ldots\ldots\ldots\ldots \textbf{(9)}$$

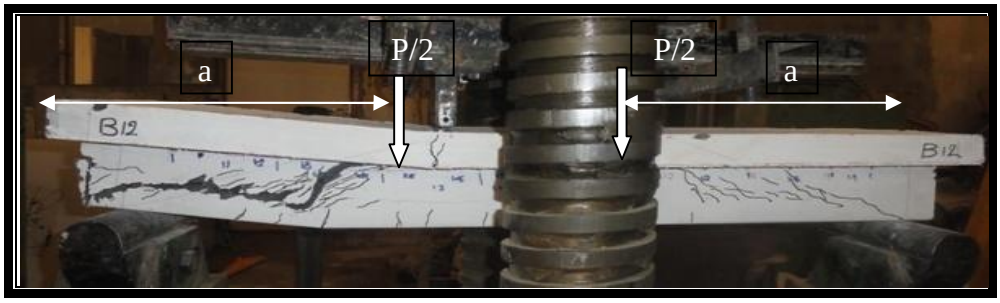

Plate .(3) : Crack Pattern of Simply Supported Test Beam under Two-Point Loading

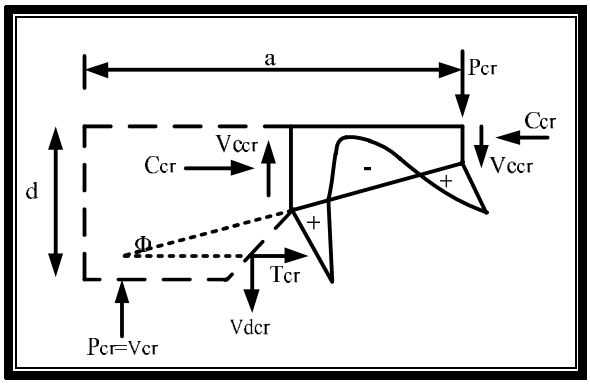

Fig .(5): Distribution of Normal Stresses along Line of Second Branch of Critical Crack [3, 4].

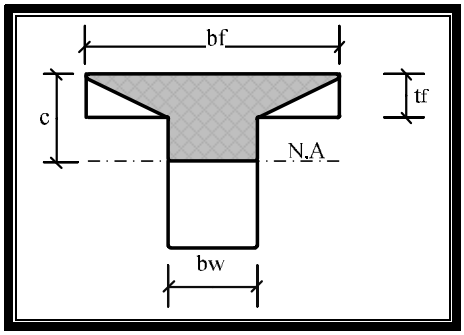

Fig .(6):Cross Section of T-Beam with Effective in Shear Area of Concrete (Shaded)[4] .

10. Proposed Equation for The Prediction of Shear Capacity of RPC T- Sections

The method presented by Zararis , L.P. and Zararis, P.D (2006)[4] for ordinary RC T-beams is modified in the present research and a new expression is established for determining the shear strength of RPC T-beams . The depth *c* of the compression zone in Eq. (8) is now determined analytically after taking into account the shape of the compression zone.

In ordinary reinforced concrete and according to ACI- Code (2008) [5], the parameter γ equals to 0.85 while β is taken as follows:

for $17 \leq f_c' \leq 28$ MPa β=0.85

for $f_c' \geq 28$ MPa $\beta = 0.85 - \frac{(f_c' - 28)}{7} 0.05 \leq 0.65$

For RPC the values of γ and β are higher than in normal concrete because these values are mainly affected by the magnitude of the concrete compressive strength and the steel fibers volumetric ratio.

Hannawayya [6] suggested new values of γ and β for RPC as shown below and these values are adopted in this work.

$$\gamma = 1 - \frac{1.71}{100}\left(f'_{cf}\, v_f\right)^{2.85} \qquad \text{..... (10)}$$

$$\beta = 0.922 - \frac{1.92}{100}\left(f'_{cf}\, v_f\right)^{3.23} \qquad \text{..... (11)}$$

In the present research, analytical study is devoted to determine the depth of the compression zone (*c*) based on modifying the simplified stress and strain distributions given by ACI committee 544[7] to read those shown in **Figure. (7).** It can be seen from this figure that the maximum useable strain at the extreme concrete compression fiber is taken to be 0.006, the concrete stress is $\gamma f'_{cf}$ and the height of the rectangular compression block is βc.

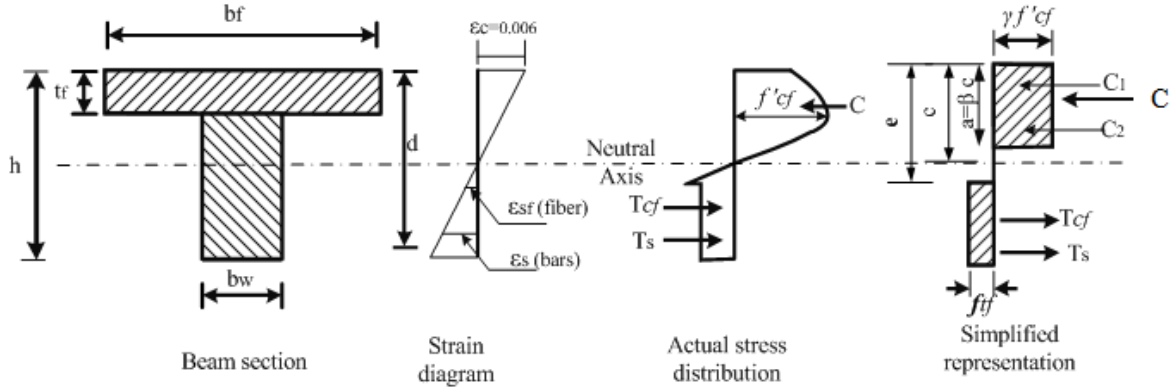

Fig .(7): Actual and Equivalent Stress Distribution for RPC T-Cross-Section.

From the stress diagram in Fig.(7) the internal forces are:

C =force in RPC in compression

$$C = C_1 + C_2$$

$$C_1 = b_f\, t_f\, \gamma\, f'_{cf}$$

$$C_2 = \left(\beta c - t_f\right) b_w\, \gamma\, f'_{cf}$$

$$C = b_f\, t_f\, \gamma\, f'_{cf} + \left(\beta c - t_f\right) b_w\, \gamma\, f'_{cf} \qquad \text{..... (12)}$$

T= force in RPC in tension

$$T = T_s + T_{cf}$$

$$T_s = A_s\, f_s$$

$$T_{cf} = f_{tf}\,(h - e)\, b_w$$

$$T = A_s\, f_s + f_{tf}\,(h - e)\, b_w \qquad \text{..... (13)}$$

For the internal forces to be in equilibrium $C = T$.

$$b_f\ t_f\ \gamma\ f'_{cf} + (\beta c - t_f)\ b_w\ \gamma\ f'_{cf} = A_s\ f_s + f_{tf}\ (h - e)\ b_w \qquad \text{..... (14)}$$

Taking into account the distribution of strain over a vertical section, **Figure.(7)**

$$A_s\ f_s = A_s\ E_s\ \varepsilon_s = \rho_w\ b_w\ d\ E_s\ \varepsilon_c \left(\frac{d - c}{c}\right)$$

Substituting these values in the previous equation of forces, after considering that $E_s\ \varepsilon_c = 2 \times 10^5 \times 0.006 = 1200$ MPa then the depth c of the compression zone is given by the positive root of the following equation

$$\left[\beta + 1.25\ \frac{f_{tf}}{\gamma f'_{cf}}\right]\left(\frac{c}{d}\right)^2 + \left[\frac{t_f}{d}\left(\frac{b_f}{b_w} - 1\right) + 600\ \frac{2\rho}{\gamma f'_{cf}} - \frac{f_{tf}}{\gamma\ f'_{cf}}\frac{h}{d}\right]\left(\frac{c}{d}\right) - 600\ \frac{2\ \rho}{\gamma f'_{cf}} = 0 \qquad \text{.....(15)}$$

where:

β = equivalent compressive stress distribution parameter.

γ = equivalent compressive stress distribution parameter.

ρ = ratio of tension reinforcement , which equals $\frac{A_s}{b_w\ d}$

e = distance from extreme compression fiber to top of tensile stress block of RPC, and is found as below, **Figure. (7)**

$$e = [\varepsilon_{sf} + 0.006] * \frac{c}{0.006} \qquad \text{..... (16)}$$

ε_{sf} = tensile strain in steel fibers $= \frac{\sigma_f}{E_s}$

σ_f = tensile strength of the fibers.

f_{tf} = tensile stress in fibrous concrete, calculated as[8]

$$f_{tf} = K_{max.}\cdot\ \alpha_f\ v_f\ \tau_b \qquad \text{..... (17)}$$

$K_{max.}$ = maximum value of the global orientation factor for the case where all fibers pullout from the matrix [8,9]

$$K_{max.} = 0.5 - \frac{0.645}{(\alpha_f)^{0.45}} \qquad \text{..... (18)}$$

$\alpha_f = \frac{l_f}{d_f}$ aspect ratio of fibers.

l_f = fiber length.

d_f = fiber diameter.

v_f = percent by volume of steel fibers**.**

τ_b = bond stress between the fibers and the concrete matrix

$$\tau_b = 0.6\sqrt{f'_{cf}} \text{ ...for straight fibers} \qquad \text{..... (19)}$$

f'_{cf} = mean compressive cylinder strength.

a = depth of rectangular stress block

b_w = width of web.

b_f = width of flange

c = distance from extreme compression fiber to neutral axis found by equating the internal tension and compression forces

d = distance from extreme compression fiber to centroid of tension reinforcement

ε_s = tensile strain in steel reinforcement.

ε_c = compressive strain in concrete

f_y = yield strength of reinforcing bar

A_s = area of tension reinforcement

C = compressive force

h = total depth of beam

E_s = modulus of elasticity of steel

T_{cf} = tensile force of fibrous concrete =f_{tf} *bw (h - e)*

T_s = tensile force of bar reinforcement = *As fy*.

In the present research, an attempt was undertaken to obtain new values of a correction factor for the size effect that can be used to calculate the shear capacity of RPC T- beams. The value of this correction factor is found to be mainly affected by the magnitude of the depth d, a/d ratio and the steel fiber volumetric ratio. Therefore, a new relation is obtained using regression analysis. The suggested value of the size effect for RPC is

$$\left(1.2 + 21.6\, v_f - 1.7\,\frac{a}{d}\,d\right) \qquad where: d \text{ in meters} \qquad \text{.....(20)}$$

Then the ultimate shear force of an RPC T-beam without shear reinforcement is:

$$V_u = \left(1.2 + 21.6\, v_f - 1.7\,\frac{a}{d}\,d\right)\frac{c}{d}\, f_{spf}\, b_{ef}\, d \qquad \text{..... (21)}$$

11. Evaluation of the Proposed Shear Capacity Equation

11.1 Comparison with Experimental Results

The accuracy of Eq. 21 can be examined through comparison with the experimental data and the results presented in **Table (6).** The comparison shows that the proposed shear capacity equation (21) gives reasonable estimated of the actual shear capacity of RPC T-

beams as determined from the present experimental tests with the mean experimental to theoretical ratios (μ) of 1.07 with standard deviation (SD) of 0.079 and coefficients of variation (COV) of 7.4 %. **Figure. (8)** shows the ultimate shear capacity obtained from the experimental work versus the corresponding theoretical value from Eq. 21, while Fig. 9 shows the ratio Vu-test/Vu-proposed versus different factors that influence *the* shear strength of RPC T-beams including f'_{spf}, f'_{cf}, ρ_w, *a/d*, *c/d* and V_f.

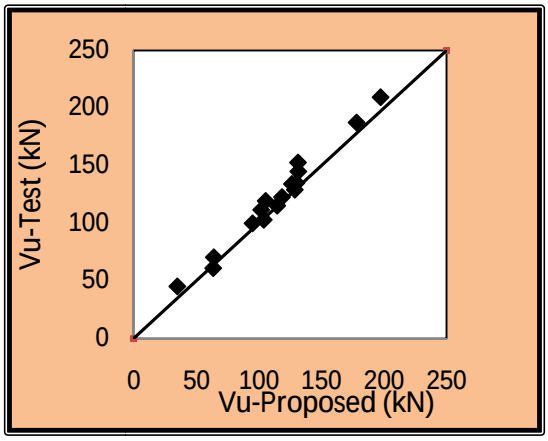

Fig .(8) Experimental Versus proposed Values for The Shear Capacity of RPC T-Beams.

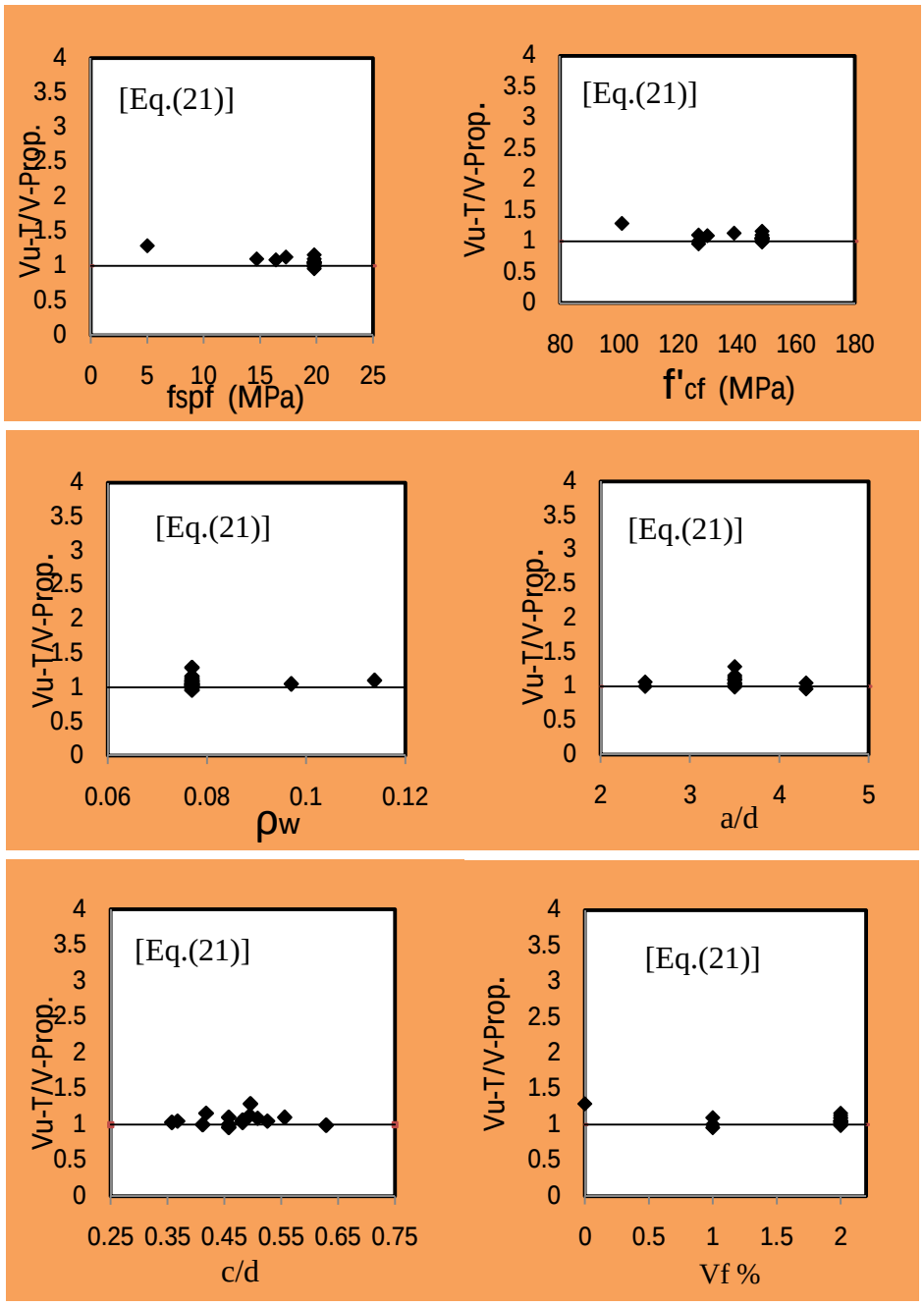

Fig .(9) The Ratio Vu-T/Vu-Proposed Versus Different Factors (f'_{spf}, f'_{cf}, ρ_w, *a/d*, *c/d* and V_f) Respectively.

11.2 Comparison with Various Design Approaches

In this section, two methods of approach for the shear design of concrete members are presented. One was given in the RILEM recommendation (2003) [10] for describing the shear behavior of steel fiber reinforced concrete (SFRC) beams and the other one was suggested by Ridha[11] (2010) for estimating the shear capacity of RPC rectangular beams. **Table (5)** shows the detail of these equations

Table .(5): Shear Capacity Equations of RPC Rectangular Beams.

Design Approaches	Proposed equations
RILEM Design Method[10]	$V_{Rd3} = V_{cd} + V_{fd}$ … (22) $V_{cd} = \left[0.12\,K\,(100\,\rho\,f'_{cf})^{\frac{1}{3}}\right] b_w\,d \quad (N)$ ….(23) $K = 1 + \sqrt{\frac{200}{d}}$ (d in mm) and K≤ 2 $V_{fd} = k_f\,K_1\,\tau_{fd}\,b_w\,d \quad (N)$ …..(24) where:k_f=factor for taking into account the contribution of the flanges in a T-section: $K_f = 1 + n\left(\frac{t_f}{b_w}\right)\left(\frac{t_f}{d}\right) \qquad K_f \le 1.5$ …..(25) with t_f is the flange thickness ; b_f is the flange width and *bw* is the web width. $n = \frac{b_f - b_w}{t_f}$ *where* $n \le 3$; $n \le \frac{3\,b_w}{t_f}$ *and* $K_1 = \frac{1600-d}{1000}$ *and* $K_1 \ge 1$ and τ_{fd} is a design value representing the increase in shear strength due to steel fiber and is taken as 0.12 *fct*.
Ridha [11]	**ACI 318M-08 modified [11] *** ***[Eq. (11-3)] modified [11]*** $V = \left[0.17\,f'_{cf} + 15\,f'_{cf}\,\rho_w\left(\frac{a}{d}\right)^{-2}(F)^{0.24}\right] b_w\,d$ ….. (26) ***[Eq. (11-5)] modified[11]*** $V = \left[0.16\,f'_{cf} + 17\rho_w\,\frac{d}{a} + 15\,f'_{cf}\,\rho_w\left(\frac{a}{d}\right)^{-2}(F)^{0.24}\right] b_w\,d$ …..(27) **Canadian Standards Association, CSA Standard CSA-A23.3- M84 modified [11] *** $V_{CAN(modified)} = \left[0.2\,f'_{cf} + 15\,f'_{cf}\,\rho_w\left(\frac{a}{d}\right)^{-2}(F)^{0.24}\right] b_w\,d$ …..(28) **British Standards Institution, BS-8110: 1997 modified [11]** $V_{BS(modified)} = \left[0.8\left\{(100\,\rho_w)^{1/3}\left(\frac{400}{d}\right)^{1/4}\left(\frac{f'_{cf}}{20}\right)^{1/3}\right\} + 15 f'_{cf}\,\rho_w\left(\frac{a}{d}\right)^{-2}(F)^{0.24}\right] b_w\,d$ …..(29)

* In all these codes, the term f'_{cf} for RPC is used to replace f'_c for ordinary RC.

The proposed equation for estimating the ultimate shear capacity of RPC T-beams as given in the present research (Eq.21) is compared with the shear capacity equation (22) given by RILEM for SFRC beams and the corresponding shear capacity equations (26 to 29) given

by Ridha as modifications to the original equations given by the different codes to read for RPC rectangular beams.

From **Table (6)**, it can be seen that the proposed Eq. (21) gives a better prediction of shear capacity in comparison with test results than the other methods. This is because RILEM method works better for shear in (SFRC) not RPC, and other equations [Eq. (26) to (29)] may be useful for shear of RPC beams with rectangular sections. Where Eq.(21) gives COV value of 7.4 percent while RILEM equation gives much higher COV value (27.4%) and the modified equations of the different codes give COV values 50.5%, 43.6% ,43.1% and 25.4% respectively .

Table .(6) Comparison of Ultimate Shear Capacity (V_u) Between Theory and Experiments.

Beam no.	Vu-T kN	Theory [Eq.(21)]		RILEM [Eq.(22)]		Modification of ACI Building Equation by Ridha [Eq.(26)]		Modification of ACI Building Equation by Ridha [Eq.(27)]		Modification of CSA-A23.3-M84 Equation by Ridha [Eq.(28)]		Modification of BS-8110:1997 Equation by Ridha [Eq.(29)]	
		Vu (kN)	Vu,T/ Vu,theo.	Vu (kN)	Vu,T/ Vu,theo.	Vu (kN)	Vu,T/ Vu, theo.	Vu (kN)	Vu,T/ Vu theo.	Vu (kN)	Vu,T/ Vu theo.	Vu (kN)	Vu,T/ Vu theo.
B1	45.25	35	1.2	48.8	0.9	21.7	2.1	25.2	1.79	25.6	1.76	45.9	0.98
B2	70.50	64.10	1.1	84.8	0.8	141.	0.5	144.3	0.48	145.3	0.48	166.2	0.42
B3	122.7	118.6	1.03	105.5	1.2	187.3	0.7	190.6	0.64	192.0	0.63	213.2	0.57
B8	209.5	197.4	1.06	105.5	1.9	341.9	0.67	347.0	0.60	346.6	0.60	367.8	0.56
B9	100.0	95.10	1.05	105.5	0.9	133.1	0.8	135.3	0.73	137.7	0.72	158.9	0.62
B6	119.2	105.5	1.13	98.1	1.2	176.2	0.7	179.5	0.66	180.7	0.65	201.8	0.59
B7	111.5	101.9	1.09	96.0	1.2	165.6	0.7	168.9	0.65	170.0	0.65	190.9	0.58
mean		1.07		1.2		0.37		0.31		0.3		0.15	
SD		0.07		0.33		0.74		0.71		0.71		0.6	
COV%		7.4		27.4		50.5		43.6		43.17		25.4	

12. Conclusions

1. The result of compression on RPC cylinders indicate that increasing the steel fibers volumetric ratio V_f and/or silica fume SF increase the compressive strength (f'_{cf}) of RPC. For the mixes used in this research, the highest compressive strength (f'_{cf}) was 148.5 MPa which was recorded for V_f = 2% and SF = 25%.
2. It was found that the addition of steel fibers to RPC mixes resulted in a higher improvement of splitting tensile strength than of compressive strength.
3. Increasing steel fibers ratio from 1 to 2% increases modulus of rupture by 303.85% while increasing silica fume content from 15 to 25% increases modulus of rupture by only 12.9%. Straight steel fibers increase tensile strength of concrete by arresting micro cracks.
4. The quantity of fibers used in the concrete mixture did not significantly affect the cracking load of RPC T-beams but had a significant influence on the rate of crack propagation and on the value of the failure load.

5. At the peak load, many fine cracks had formed in the web, with the cracks well distributed through the shear spans. The failure loads of RPC T-beams, were more than twice the cracking loads.
6. Decreasing the silica fume content SF from 25% to 20% and 15%, in RPC T- beams decreased the diagonal cracking load by 6.25% and 12.5% respectively and the ultimate load by 3% and 9.2% respectively.
7. Increasing the silica fume content SF from 15% to 20% and 25% in RPC T-beams having V_f= 2% showed a lesser maximum crack width at a specific load level beyond the cracking load.
8. Increasing the shear span to effective depth ratio a/d from 2.5 to 3.5 and 4.5 in RPC T-beams having V_f= 2% and ρ_w = 7.7%decreased both diagonal crack load by 11.11% and 33.33% respectively and the ultimate load by 41.4% and 52.3% respectively.
9. The equation derived for the predication of the ultimate shear capacity (***Vu***) of RPC T-sections based on regression analysis showed good results with all the available and present experimental test results. Therefore, it can be used safely and with good accuracy in the analysis and design of RPC T-beams.

13. Reference

1. **Bonneau, O., Poulin, C., Dugat, J., Richard, P., and Aitcin, "Reactive Powder Concretes: From Theory to Practice", Concrete International, Vol. 18, No. 4, April 1999, pp. 37-39.**
2. **Iraqi Specification, No. 5/1984., "Portland cement".**
   وزارة التخطيط ،الجهاز المركزي للتقييس والسيطرة النوعية.
3. **P. D. Zararis and G. Ch. Papadakis, "Diagonal Shear Failure and Size Effect in Rc Beams without Web Reinforcement" , Journal of Structural Engineering , July 2001 , pp. 733-742.**
4. **Zararis I. P., Maria k. Karaveziroglou, and Prodromos D. Zararis,''Shear Strength of Reinforced Concrete T-Beams'', ACI Structural Journal, V. 103, No. 5, September-October 2006, pp. 693-699.**
5. **ACI Committee 318M-318RM, "Building Code Requirements for Structural Concrete and Commentary", American Concrete Institute, Farmington Hills, Michigan, 2008, 473p.**
6. **Hannawayya, S. PH. Y., "Behavior of Reactive Powder Concrete Beams in Bending", Ph.D. Thesis, University of Technology, Baghdad, 2010, 239 pp.**
7. **ACI 544.4R-88, "Design Consideration for Steel Fiber Reinforced Concrete", American Concrete Institute, Farmington Hills, Michigan, 1988, 18p**
8. **Foster, S. J., Voo, Y. L., and Chong, K. T., "FE Analysis of Steel Fiber Reinforced Concrete Beams Failing in Shear: Variable Engagement Model", ACI SP-237, Detroit, 2006, pp. 55–70.**

9. **Y. L. Voo, W. K. Poon, and Stephen J. Foster , "Shear Strength of Steel Fiber-Reinforced Ultrahigh-Performance Concrete Beams without Stirrups" , Journal of Structural Engineering, Vol. 136, No. 11, November 1, 2010, pp. 1393–1400.**
10. **RILEM TC 162-TDF: "Test and design methods for steel fiber reinforced concrete" , σ- ε design method ,Final Recommendation, Materials and Structures, Vol. 36, October 2003, pp. 560-567.**
11. **Ridha, M., M.M., "Shear Behavior of Reactive Powder Concrete Beams", Ph.D. Thesis, University of Technology, Baghdad, Iraq, 2010, 205 p.**

Appendix

Selected Data from other Literature for Compressive Strength of RPC.

Reference	*Fiber Type*	l_f *(mm)*	d_f *(mm)*	V_f%	B_f	*F*	f'_c*(MPa)*	f'_{cf} *(MPa)*
Soon,H.Ch. and Yoon, I.K	HS	36	0.6	0.5	0.75	0.225	85.2	86.1
	HS	36	0.6	1.0	0.75	0.45	85.2	89.4
	HS	36	0.6	1.5	0.75	0.675	85.2	87.7
	HS	36	0.6	2.0	0.75	0.9	85.2	89.9
	HS	36	0.6	0.5	0.75	0.225	65.3	70.5
	HS	36	0.6	1.0	0.75	0.45	65.3	67.3
	HS	36	0.6	1.5	0.75	0.675	65.3	67.3
	HS	36	0.6	2.0	0.75	0.9	65.3	69.6
	HS	36	0.6	0.5	0.75	0.225	74.1	82.4
	HS	36	0.6	1.0	0.75	0.45	74.1	81.1
	HS	36	0.6	1.5	0.75	0.675	74.1	83
	HS	36	0.6	2.0	0.75	0.9	74.1	82.2
Khuntia, M.and Stojadinovic, B.	HS	50	0.8	0.5	0.75	0.234	62.6	63.8
	HS	50	0.8	0.75	0.75	0.351	62.6	68.6
Al-Jumaily I. A. S	HS	20	0.4	1.0	0.75	0.375	99.8	110
	HS	20	0.4	2.0	0.75	0.75	99.8	120
	HS	20	0.4	1.0	0.75	0.375	82.55	89.5
	HS	20	0.4	2.0	0.75	0.75	82.55	97.6
	HS	20	0.4	1.0	0.75	0.375	63.55	69.5
	HS	20	0.4	2.0	0.75	0.75	63.55	76.06
Metin,I. et al	SS	6	0.16	2.0	0.5	0.375	125.63	154.83
	SS	6	0.16	4.0	0.5	0.75	125.63	170.29

	SS	6	0.16	6.0	0.5	1.125	125.63	181.52
	SS	6	0.16	8.0	0.5	1.5	125.63	206.74
	SS	6	0.16	10.0	0.5	1.875	125.63	230.28
Gai, F. et al	SS	13	0.4	2.0	0.5	0.325	106	151
	SS	13	0.4	2.0	0.5	0.325	100	114
	SS	13	0.4	2.0	0.5	0.325	106	139
Schmidt, M. et al	SS	5.5	0.15	2.5	0.5	0.458	190	198
Bonneau, O . et al	SS	13	0.16	1.0	0.5	0.406	163	217
	SS	13	0.16	2.0	0.5	0.8125	163	197
Maroliya, Mr. M. K.	SS	13	0.2	2.0	0.5	0.65	106	114
	SS	13	0.2	1.0	0.5	0.325	106	129
	SS	13	0.2	2.0	0.5	0.65	106	151
Abd Al-Hussein, A. J	HS	30	0.375	1.0	0.75	0.6	106	114.2
	HS	30	0.375	1.0	0.75	0.6	106	115.2
	HS	30	0.375	1.0	0.75	0.6	106	109.6
	HS	30	0.375	1.0	0.75	0.6	106	112.3
Barragán, B. E.	HS	60	0.75	2.0	0.75	1.2	77.7	76.5
	HS	60	0.75	4.0	0.75	2.4	77.7	77.8
Graybeal, B., and Davis, M.	SS			2.0	0.5	0.65	155.2	189.1
	SS			2.0	0.5	0.65	155.2	190.9
	SS			2.0	0.5	0.65	170.3	197.8
	SS			2.0	0.5	0.65	170.3	198.5
	SS			2.0	0.5	0.65	157	203.7
	SS			2.0	0.5	0.65	157	199.3
	SS			2.0	0.5	0.65	148.4	186.6
	SS			2.0	0.5	0.65	148.4	170.8
	SS			2.0	0.5	0.65	143	182.6
	SS			2.0	0.5	0.65	143	176.8
	SS			2.0	0.5	0.65	143.3	197.3
	SS			2.0	0.5	0.65	143.3	179.9
Cwirzen, A. et al	SS			2.0	0.5	1.2	184	202
	SS			3.0	0.5	1.8	176	202
Yang, J. U. et al	SS			1.0	0.5	0.325	155.97	166.27
	SS			1.5	0.5	0.487	155.97	173.73
	SS			2.0	0.5	0.65	155.97	176.3
	SS			3.0	0.5	0.975	155.97	179.17

Al-Ne'aime, S.S.H	SS			2.0	0.5	0.72	95.76	109.25
	SS			2.0	0.5	0.72	128	133.48
	SS			2.0	0.5	0.812	163	217
Menefy, L	SS	12	0.15	2.0	0.5	0.8	116.7	152.5
	SS	12	0.2	3.0	0.5	0.9	117.4	156.5
	SS	12	0.2	2.0	0.5	0.6	119.5	152.5
	SS	12	0.18	3.0	0.5	1	120.1	153.5
	SS	12	0.18	2.0	0.5	0.666	116.7	140
	SS	12	0.16	3.0	0.5	1.125	117.4	138.5
	SS	12	0.175	2.0	0.5	0.685	119.5	143
	SS	12	0.175	3.0	0.5	1.028	120.1	140
	SS	12	0.175	2.0	0.5	0.685	128	130
Hannawayya, S. PH. Y.	SS	13	0.2	1.0	0.5	0.325	79.42	99.53
	SS	13	0.2	0.5	0.5	0.1625	79.42	83.11
	SS	13	0.2	1.5	0.5	0.487	79.42	102.2
	SS	13	0.2	2.0	0.5	0.65	79.42	109.65
	SS	13	0.2	2.0	0.5	0.65	79.42	104.66
	SS	13	0.2	2.0	0.5	0.65	79.42	94.41
Ridha, M., M.M.	SS	13	0.2	2.0	0.5	0.65	78	94
	SS	13	0.2	1.0	0.5	0.325	78	98
	SS	13	0.2	1.5	0.5	0.487	78	103
	SS	13	0.2	2.0	0.5	0.65	78	110
	SS	13	0.2	2.0	0.5	0.65	78	101
	SS	13	0.2	2.0	0.5	0.65	78	93.4

Selected Data from other Literature for Splitting Tensile Strength of RPC.

Reference	*Fiber Type*	l_f *(mm)*	d_f *(mm)*	V_f%	*Bf*	*F*	*fc'(MP)*	*f'cf (MPa)*	f_{spf} *(MP)*
Voo, J.Y. **et al**	SS	13	0.2	1.25	0.5	0.406		135	12.6
	HS	35	0.43	2	0.75	1.220		162	22
	HS	35	0.43	1	0.75	0.610		150	
	HS	35	0.43	2	0.75	1.220		162	22
	SS	13	0.2	2.5	0.5	0.812		144	16.6
	SS	13	0.2	3.7	0.5	1.202		158	22.3
Khuntia, M. **et al**	HS	50	0.8	0.5	0.75	0.234	62.6	63.8	5.88
	HS	50	0.8	0.75	0.75	0.351	62.6	68.6	6.08

Mahesh, K. and Chetan, D.	SS	13	0.4	2	0.5	0.325	106	151	29
	SS	13	0.4	2	0.5	0.325	100	114	16
	SS	13	0.4	2	0.5	0.325	106	139	19
Abd Al-Hussein, A. J	HS	30	0.375	1	0.75	0.6	106	114.2	12.42
	HS	30	0.375	1	0.75	0.6	106	115.2	9.55
	HS	30	0.375	1	0.75	0.6	106	109.6	11.64
	HS	30	0.375	1	0.75	0.6	106	112.3	12.1
Menefy, L	SS	12	0.15	2	0.5	0.8	116.7	152.5	15.5
	SS	12	0.2	3	0.5	0.9	117.4	156.5	20.5
	SS	12	0.2	2	0.5	0.6	119.5	152.5	17.5
	SS	12	0.18	3	0.5	1	120.1	153.5	20
	SS	12	0.18	2	0.5	0.667	116.7	140	18
	SS	12	0.16	3	0.5	1.125	117.4	138.5	20
	SS	12	0.175	2	0.5	0.685	119.5	143	15.6
	SS	12	0.175	3	0.5	1.028	120.1	140	15
	SS	13	0.2	1	0.5	0.325	101	127	15.3
	SS	13	0.2	2	0.5	0.65	101	148.5	19.8
	SS	13	0.2	2	0.5	0.65	101	130	16.4
	SS	13	0.2	2	0.5	0.65	101	139	17.3
Ridha, M., M.M	SS	13	0.2	0.5	0.5	0.162	78	94	9.2
	SS	13	0.2	1	0.5	0.325	78	98	11
	SS	13	0.2	1.5	0.5	0.487	78	103	14.5
	SS	13	0.2	2	0.5	0.65	78	110	15.4
	SS	13	0.2	2	0.5	0.65	78	101	14
	SS	13	0.2	2	0.5	0.65	78	93.4	12.7
Voo, Y. L., Foster, S. J	SS	l/d=65		2.5	0.5	0.775		161	19.2
	SS	65		2.5	0.5	0.775		160	20.9
	SS	65		2.5	0.5	0.775		149	21.9
	SS	65		1.25	0.5	0.387		164	18
	HS	60		2.5	0.75	0.915		171	22.4
	HS	60		2.5	0.75	1.125		157	18.3
	SS	60		2.5	0.75	0.862		169	23.5
Voo, J. Y. L., Foster, S. J., Gilbert	SS	65		2	0.5	0.65		162	22
Yang, J. U. **et al**	SS	65		1	0.5	0.325	155.97	166.27	14.67
	SS	65		1.5	0.5	0.487	155.97	173.73	18.63
		65		3	0.5	0.975	155.97	179.17	22.53
Al-Ne'aime, S.S.H		72		2	0.5	0.72	95.76	112.8	17.56
		72		2	0.5	0.72	128	142	18.3
Hannawayya, S. PH. Y.	SS	13	0.2	0.5	0.5	0.162	79.42	83.11	9.16
	SS	13	0.2	1	0.5	0.325	79.42	99.53	11.01
	SS	13	0.2	1.5	0.5	0.487	79.42	102.2	14.49

	SS	13	0.2	2	0.5	0.65	79.42	109.65	14.44
	SS	13	0.2	2	0.5	0.65	79.42	104.66	14.14
	SS	13	0.2	2	0.5	0.65	79.42	94.41	12.66

Selected Data from other Literature for Modulus of Rupture of RPC.

Reference	*Fiber Type*	l_f *(mm)*	d_f *(mm)*	V_f%	B_f	*F*	*fc'(MPa)*	f'_{cf} *(MPa)*	f_r *(MPa)*
Soon,H.Ch. and Yoon, I.K.	HS	36	0.6	0.5	0.75	0.225	85.2	86.1	5.46
	HS	36	0.6	1.0	0.75	0.450	85.2	89.4	6.44
	HS	36	0.6	1.5	0.75	0.675	85.2	82.7	7.09
	HS	36	0.6	2.0	0.75	0.900	85.2	89.9	7.54
	HS	36	0.6	0.5	0.75	0.225	65.3	70.5	5.27
	HS	36	0.6	1.0	0.75	0.450	65.3	67.3	5.27
	HS	36	0.6	1.5	0.75	0.675	65.3	67.3	5.20
	HS	36	0.6	2.0	0.75	0.900	65.3	69.6	6.96
	HS	36	0.6	0.5	0.75	0.225	74.1	82.4	5.27
	HS	36	0.6	1.0	0.75	0.450	74.1	81.1	6.44
	HS	36	0.6	1.5	0.75	0.675	74.1	83	7.54
	HS	36	0.6	2.0	0.75	0.900	74.1	82.2	8.06
Khuntia, M. **et al**	HS	50	0.8	0.5	0.75	0.234	62.6	63.8	10.10
	HS	50	0.8	0.75	0.75	0.351	62.6	68.6	10.69
Al-Jumaily I. A. S.	HS	20	0.4	1.0	0.75	0.375	99.8	110	15.52
	HS	20	0.4	2.0	0.75	0.750	99.8	120	16.39
	HS	20	0.4	1.0	0.75	0.375	82.55	89.5	13.11
	HS	20	0.4	2.0	0.75	0.750	82.55	97.6	13.86
	HS	20	0.4	1.0	0.75	0.375	63.55	69.5	10.25
	HS	20	0.4	2.0	0.75	0.750	63.55	76.06	10.86
Mahesh, K. and Chetan, D.	SS	13	0.4	2.0	0.5	0.325	106	151	
	SS	13	0.4	2.0	0.5	0.325	100	114	22.0
	SS	13	0.4	2.0	0.5	0.325	106	139	27.50
Maroliya, Mr. M. K.	SS	13	0.2	2.0	0.5	0.650	106	114	17.50
	SS	13	0.2	1.0	0.5	0.325	106	129	19.0
	SS	13	0.2	2.0	0.5	0.650	106	151	29.0
Abd Al-Hussein, A. J.	HS	30	0.375	1.0	0.75	0.600	106	114.2	14.40
	HS	30	0.375	1.0	0.75	0.600	106	115.2	14.85
	HS	30	0.375	1.0	0.75	0.600	106	109.6	16.20
	HS	30	0.375	1.0	0.75	0.600	106	112.3	15.57

Menefy, L.	SS	12	0.15	2.0	0.5	0.800	116.7	152.5	7.40
	SS	12	0.2	3.0	0.5	0.900	117.4	156.5	7.50
	SS	12	0.2	2.0	0.5	0.600	119.5	152.5	7.40
	SS	12	0.18	3.0	0.5	1.000	120.1	153.5	7.40
	SS	12	0.18	2.0	0.5	0.667	116.7	140	7.099
	SS	12	0.16	3.0	0.5	1.125	117.4	138.5	7.06
	SS	12	0.175	2.0	0.5	0.685	119.5	143	7.175
	SS	12	0.175	3.0	0.5	1.028	120.1	140	7.099
	SS	12	0.175	2.0	0.5	0.685	128	130	6.84
	SS	13	0.2	1.0	0.5	0.325	101	127	14.10
	SS	13	0.2	2.0	0.5	0.650	101	148.5	21.00
	SS	13	0.2	2.0	0.5	0.650	101	130	18.60
	SS	13	0.2	2.0	0.5	0.650	101	139	19.0
Ridha, M., M.M.	SS	13	0.2	0.5	0.5	0.162	78	94	10.00
	SS	13	0.2	1.0	0.5	0.325	78	98	12.00
	SS	13	0.2	1.5	0.5	0.487	78	103	15.05
	SS	13	0.2	2.0	0.5	0.650	78	110	19.00
	SS	13	0.2	2.0	0.5	0.650	78	101	17.60
	SS	13	0.2	2.0	0.5	0.650	78	93.4	16.00
Hannawayya, S. PH. Y.	SS	13	0.2	0.5	0.5	0.162	79.42	83.11	7.55
	SS	13	0.2	1.0	0.5	0.325	79.42	99.53	9.20
	SS	13	0.2	1.5	0.5	0.487	79.42	102.2	15.05
	SS	13	0.2	2.0	0.5	0.650	79.42	109.65	19.00
	SS	13	0.2	2.0	0.5	0.650	79.42	104.66	18.70
	SS	13	0.2	2.0	0.5	0.650	79.42	94.41	17.62
Voo, J.Y. **et al**	SS			2.5	0.5	0.775		161	29.80
	SS			2.5	0.5	0.775		160	26.40
	SS			2.5	0.5	0.775		149	23.20
	SS			1.25	0.5	0.387		164	14.80
	HS			2.5	0.75	0.915		171	26.30
	HS			2.5	0.75	1.125		157	25.20
	HS			2.5	0.75	0.862		169	23.80
Wen-yu, J. **et al**	SS			2.0	0.5	0.650		166.9	20.60
	SS			2.0	0.5	0.650		145.8	21.10
Fujikake, K. **et al**				2.0	0.5	0.750		214.7	40.00
Gao, R., Stroeven, P., and Hendriks, C. F	SS			2.0	0.5	0.590		168.6	20.60

Voo, J. Y. L., Foster, S. J.	SS			2.0	0.5	0.650		162	20.00
Cwirzen, A., Penttala, V., Vornanen, C.	SS			2.0	0.5	1.200	184	202	26.00
	SS			3.0	0.5	1.800	176	202	36.00
Yang, J. U. et al	SS			1.0	0.5	0.325	155	166.2	16.65
	SS			1.5	0.5	0.487	155	173.7	22.71
	SS			2.0	0.5	0.650	155	176.3	28.05
	SS			3.0	0.5	0.975	155	179.1	34.51

Fiber Type: HS = hooked ends steel
SS = straight steel